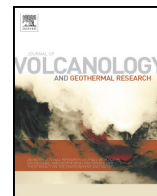




Contents lists available at ScienceDirect

Journal of Volcanology and Geothermal Research

journal homepage: www.elsevier.com/locate/jvolgeores

Remote sensing and petrological observations on the 2012–2013 fissure eruption at Tolbachik volcano, Kamchatka: Implications for reconstruction of the eruption chronology

Dmitry Melnikov*, Anna O. Volynets

Institute of Volcanology and Seismology FEB RAS, Piip Boulevard 9, Petropavlovsk-Kamchatsky 683006, Russian Federation

ARTICLE INFO

Article history:

Received 14 February 2015

Accepted 29 September 2015

Available online xxxx

Keywords:

Kamchatka

Tolbachik volcano

Monogenetic volcanism

Remote sensing

Volcanic ash

Suomi NPP VIIRS

ABSTRACT

We present a reconstruction of the chronological sequence of events that took place during the first days of the 2012–2013 Tolbachik fissure eruption using petrological data and remote sensing methods. We were forced to use this approach because bad weather conditions did not allow direct observations during the first two days of the eruption. We interpreted infrared images from the scanning radiometer VIIRS Suomi NPP and correlated the output with the results of the geochemical study, including comparison of the ash, deposited at the period from 27 to 29 November, with the samples of lava and bombs erupted from the Menyailov and Naboko vents. We argue that the compositional change observed in the eruption products (the decrease of SiO₂ concentration and K₂O/MgO ratio, increase of MgO concentration and Mg#) started approximately 24 h after the eruption began. At this time the center of activity moved to the southern part of the fissure, where the Naboko group of vents was formed; therefore, this timeframe also characterizes the timing of the Naboko vent opening. The Naboko group of vents remained active until the end of eruption in September 2013.

© 2015 Elsevier B.V. All rights reserved.

1. Introduction

Tolbachinsky Dol (TD) is located at the northern part of the Kamchatka island arc system and belongs to the Klyuchevskoy group of volcanoes (Churikova et al., 2015; in this issue). It comprises lava flows and pyroclastic deposits produced by numerous scoria cones formed along the regional linear fault zone about 70 km long. At its northern end Tolbachinsky Dol crosses Ostry and Plosky Tolbachik stratovolcanoes. About 80% of the TD eruptive centers are concentrated along the narrow axial part of this regional fault zone. In the Holocene, more than 60 eruptions took place in TD (Fig. 1, Fedotov, 1983; Fedotov et al., 1984). Historical eruptions produced Krasny and Zvezda scoria cones (1740 CE), the 1941 CE cone, and the Northern and Southern Breakthroughs of the 1975–76 Tolbachik Fissure eruption (Fedotov, 1983; Fedotov et al., 1984; Inbar et al., 2011). On 27 November 2012, after minor precursory seismicity (Senyukov et al., in this issue; Kugaenko et al., in this issue; Kugaenko et al., 2014) a new eruption began on the southern slope of Plosky Tolbachik stratovolcano. At the beginning, a 6 km long sub-meridional fissure was formed; its opening was accompanied by intense lava effusion. Later, explosive and effusive activity was concentrated at two centers: Menyailov vent at the northern part of the fissure, and Naboko vent at the southern part of the

fissure. The lava discharge rate during the first two days was ~440 m³/s, and by 29 November 2012 lava flows covered an area of 14.46 km² (Dvigalo et al., 2014). By 30 November the activity of the Menyailov group of vents ceased. From this point until the end of eruption in September 2013, the activity was concentrated at the Naboko group of vents. Unfortunately, on 27–28 November 2012 a strong snowstorm above Kamchatka prevented direct observation of the beginning of the eruption; thus no visual observations exist to confirm the exact time of the beginning of the Naboko vents' activity. Here we make an attempt to reconstruct the eruption chronology during the period of 27–30 November, using satellite and petrological data.

2. Data and methods

2.1. Satellite data

Based on seismic data, the 2012–2013 Tolbachik fissure eruption (FTE) started at 05:15 UTC 27 November 2012 (Senyukov et al., 2015; in this issue). Cloud cover and a snowstorm at this time made visual ground-based and satellite-based observations impossible. Satellite images did not record ash clouds. Only 11 h later (at 16:30 UTC 27 November 2012) an AIRS satellite image showed an SO₂-bearing cloud (according to the data of Support to Aviation Control Service <http://sacs.aeronomie.be>; Brenot et al., 2014), which was located about 800 km to the north of the eruption site. Most likely, this cloud corresponds to the first explosive phase of the fissure opening at the

* Corresponding author at: Institute of volcanology and seismology FEB RAS, Piip boulevard 9, Petropavlovsk-Kamchatsky 683006, Russia.

E-mail address: dvm@kscnet.ru (D. Melnikov).

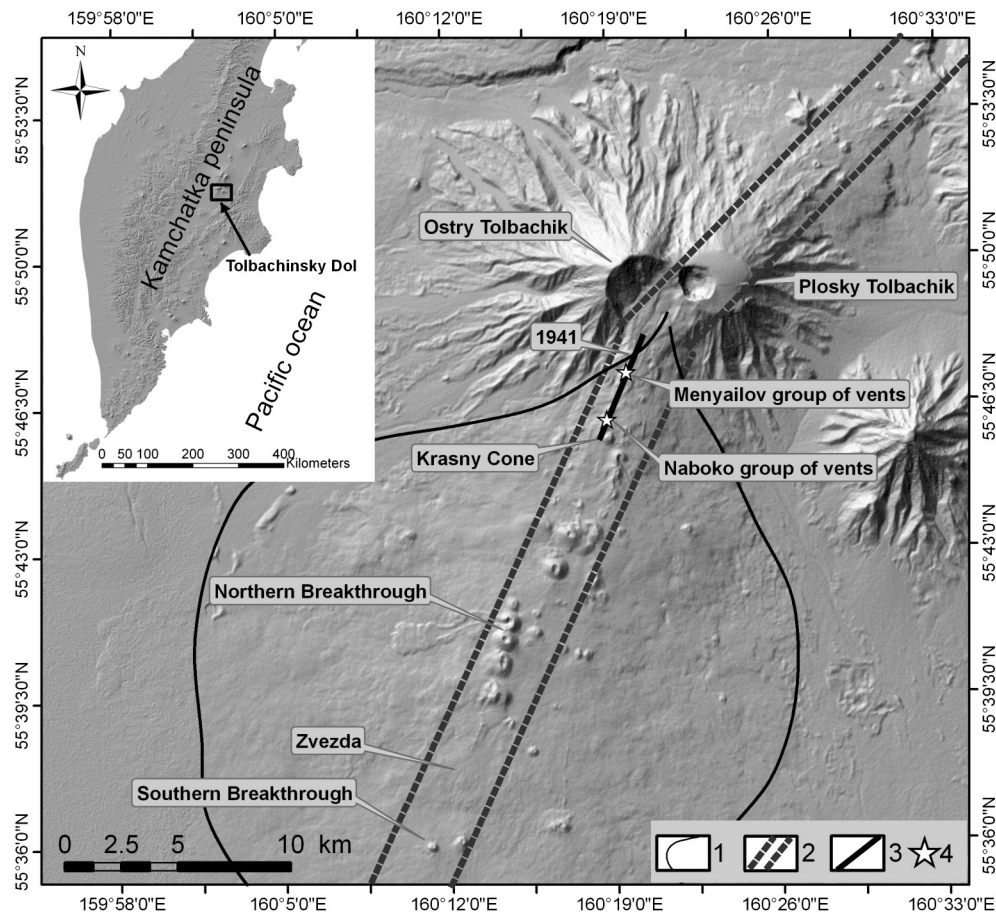


Fig. 1. Schematic map of Tolbachinsky Dol and its location in the Kamchatka arc system. Legend: 1—the boundary of Tolbachinsky Dol; 2—regional linear fault zone; 3—fissure zone of the 2012–2013 Tolbachik fissure eruption; 4—Menyailov group of vents and Naboko group of vents. Centers of the historical eruptions are outlined as follows: Northern and Southern Breakthroughs of the 1975–76 Tolbachik fissure eruption; cinder cone of the 1941 CE eruption; Krasny cinder cone and Zvezda eruptive center (1740 CE). The topographic base is a DEM-derived from SRTM X-band (DLR).

Menyailov vent. After that, the seismic data (Senyukov et al., 2015) indicate a decrease in activity, followed by the strong volcanic tremor at ~08:00 UTC 27 November 2012, possibly caused by the onset of intense lava effusion.

Infrared satellite images of various spatial resolutions are now routinely used for the analyses of lava flows dynamics (Harris et al., 1998; Pieri and Abrams, 2004; Harris, 2013; Wright et al., 2015). High-resolution satellite images (TERRA ASTER, EO-1 ALI), where the lava flows could be viewed in detail, are available for the FTE area only from the beginning of December 2012. For the period from 27 to 30 November 2012, only low-resolution satellite data from MODIS, and AVHRR are available with the spatial resolution for the IR channel of ~1 km/pixel. This kind of resolution is not suitable for the analyses of FTE lava flows. For more detailed analyses of the morphology and edges of the lava flows we used data from the Visible Infrared Imaging Radiometer Suite (VIIRS), which is located on the Suomi NPP satellite and provides global coverage of the Earth's surface every 12 h. One advantage of VIIRS is that it has two infrared channels with spatial resolution 375 m. VIIRS I4 has a channel for wavelengths between 3.55 and 3.93 μm with a pixel saturation temperature of 367 K; additionally, when pixel saturation is associated with intensive heat flow (large wildfires, lava flows) the pixel's brightness temperature may be set at 208 K (Schroeder et al., 2014). There is also an I5 channel for wavelengths between 10.5 and 12.4 μm and a saturation temperature of 380 K. It has been previously shown that these channels provide good results for the detection and description of active fires and their morphologies (Schroeder et al., 2014). Raw satellite images were obtained through

the Comprehensive Large Array-data Stewardship System (<http://www.nsof.class.noaa.gov>) as Level1 Sensor Data Records (SDR) files.

2.2. Geochemical data

Three samples of ash, produced during the first days of the eruption, were chosen for geochemical analyses; the results were compared with the comprehensive data set of the representative collection of rocks that characterize the composition of lava from the first until the last day of the eruption (Volynets et al., in this issue; Volynets et al., 2013). Concentrations of the major and selected trace elements (V, Cr, Co, Ni, Cu, Zn, Rb, Sr, Y, Zr, Nb, Ba, Pb) in these three ash samples were analyzed by X-ray fluorescence spectroscopy (XRF) using an Axios MAX vacuum sequential spectrometer (wavelength dispersive) by PANalytical at the Institute of Geology of Ore Deposits, Petrography, Mineralogy, and Geochemistry, Russian Academy of Sciences (IGEM RAS). Descriptions of the sample preparation methods and analytical errors are provided in Volynets et al. (2015; in this issue).

3. Results

3.1. Satellite data

Fig. 2 shows images from the I4 and I5 channels at brightness temperature (in Kelvin). The first image, showing a thermal anomaly above the eruption area, was made at 15:30 UTC 27 November 2012, but the anomaly is visible only with I4 channel, because clouds prevent

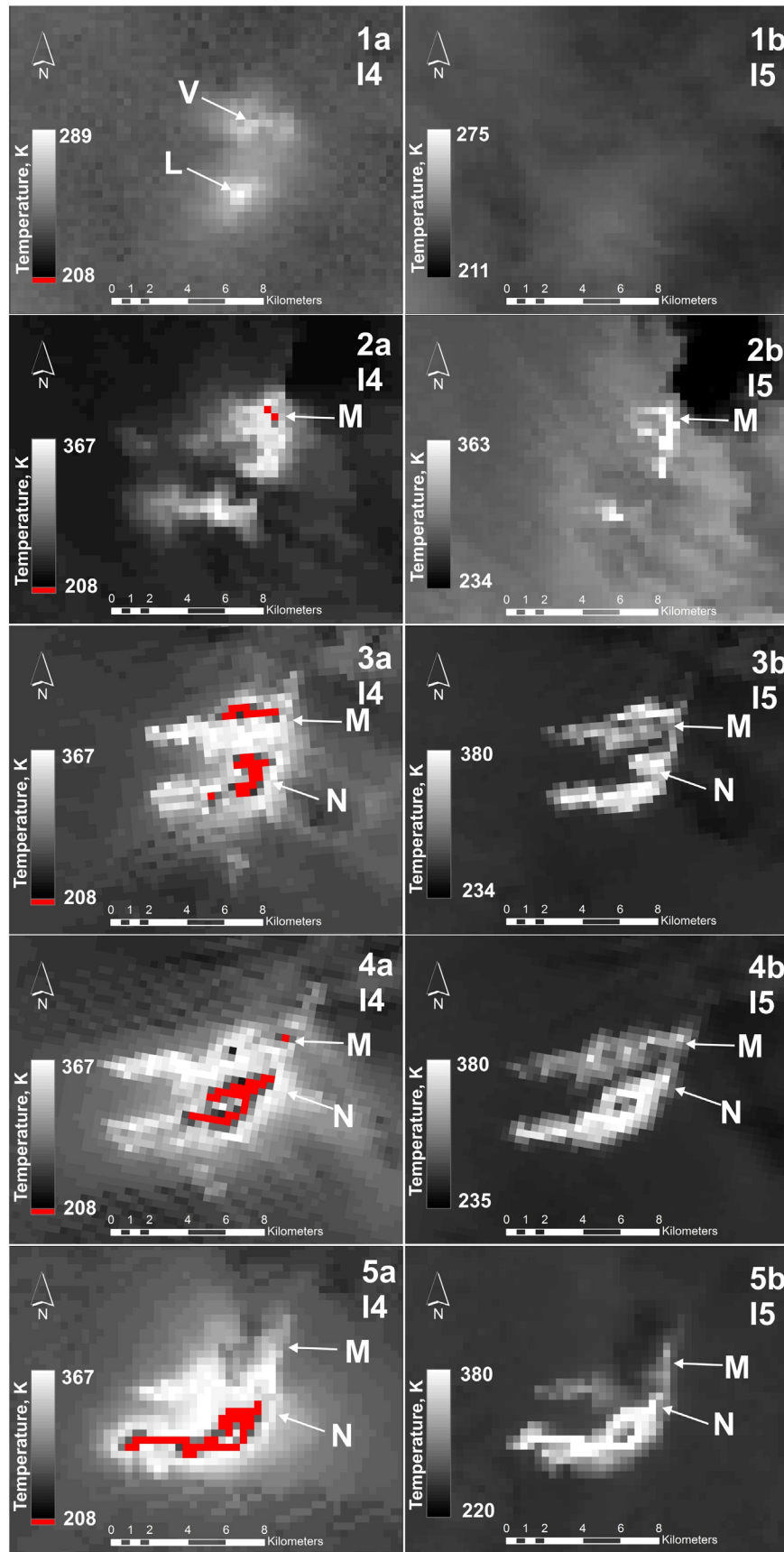


Fig. 2. Thermal images from I4 (a) and I5 (b) channels from the scanning radiometer VIIRS Suomi NPP. Images were collected at the following times: 1a–1b 15:30 UTC 27 November 2012; 2a–2b 15:12 UTC 28 November 2012; 3a–3b 00:58 UTC 29 November 2012; 4a–4b 02:40 UTC 29 November 2012; 5a–5b 14:49 UTC 29 November 2012. Letters and arrows indicate: V and L—Vodopadny and Leningradsky lava flows; M—Menyailov group of vents; N—Naboko group of vents. Red pixels at I4 channel images correspond to the temperatures exceeding saturation level and characterize the hottest parts of the lava flows. (For interpretation of the references to color in this figure legend, the reader is referred to the web version of this article.)

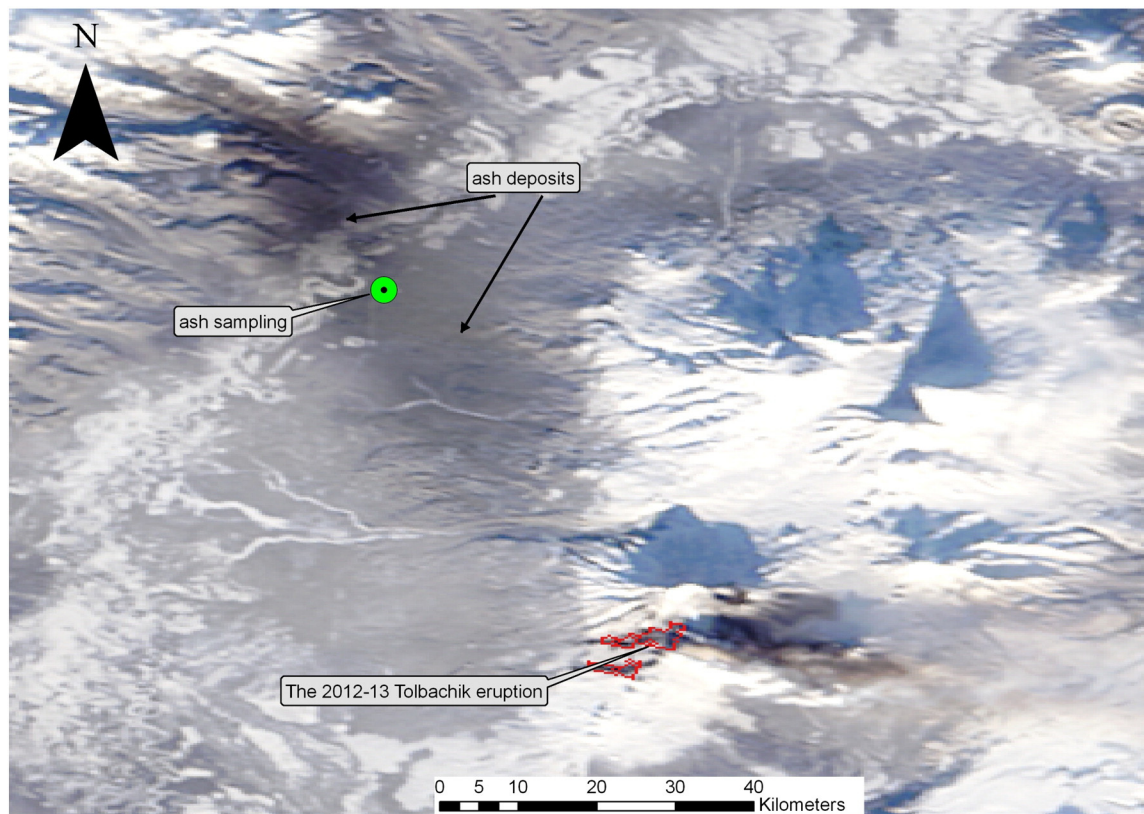


Fig. 3. MODIS Aqua 02:50 UTC 29 November 2012 (<http://lance-modis.eosdis.nasa.gov>) satellite image. The area influenced by the ash deposition is clearly seen to the northwestern direction from FTE. Asterisk marks sampling site location.

the detection of this thermal anomaly at I5 channel. Data from the I4 channel shows two bright thermal anomalies, which correspond to the two lava flows—Vodopadny and Leningradsky (Belousov et al., 2015; in this issue). Heavy cloud cover does not allow for an exact evaluation of the extent of the lava flows. The next image was taken at 15:12 UTC 28 November 2012, after the snowstorm above Klyuchevskoy group of volcanoes ended and more detailed observations then became possible. At this time thermal anomalies are observed at both channels, I4 and I5. On the I4 channel two pixels lying above the saturation level correspond to the intensive explosive and effusive processes at the Menyailov group of vents. This zone is visible also on the I5 channel. The following satellite images were made at 00:58, 02:40 and 14:49 UTC 29 November 2012. They show a gradual decrease in the intensity of the thermal anomaly above the Menyailov vent, and, an increase of the amount of pixels with high temperature above the Naboko group of vents. Morphologically, the thermal anomaly at the Naboko group of vents has an elongated form; that corresponds to the movement of the fresh lava flow. On the I4 channel pixels exceeding the saturation level correspond to this lava flow. This lava flow was produced on the southernmost part of the FTE fissure zone, which intersected Krasny cone (formed in 1740 CE). Therefore, based on the remote sensing data, the effusive activity at FTE on the afternoon of 29 November 2012 (UTC) was already concentrated mostly within the Naboko group of vents.

3.2. Geochemical composition of the ash samples

A typical feature of the new eruption was its effusive character. The volume explosivity coefficient (the volume ratio of the pyroclastics to lava) is about 3% (Gordeev et al., 2013). Most likely, the first explosion accompanying the fissure opening, was the biggest. The ash was deposited to the north and northwest from the volcano. Its density was up to 500 g/m² (Gordeev et al., 2013). The maximum thickness of ash was

observed about 60 km to the northwest from the FTE, in the Mayskoe village area where the ash samples were collected. The ash fallout zone is visible on the MODIS Aqua satellite image at 02:50 UTC 29

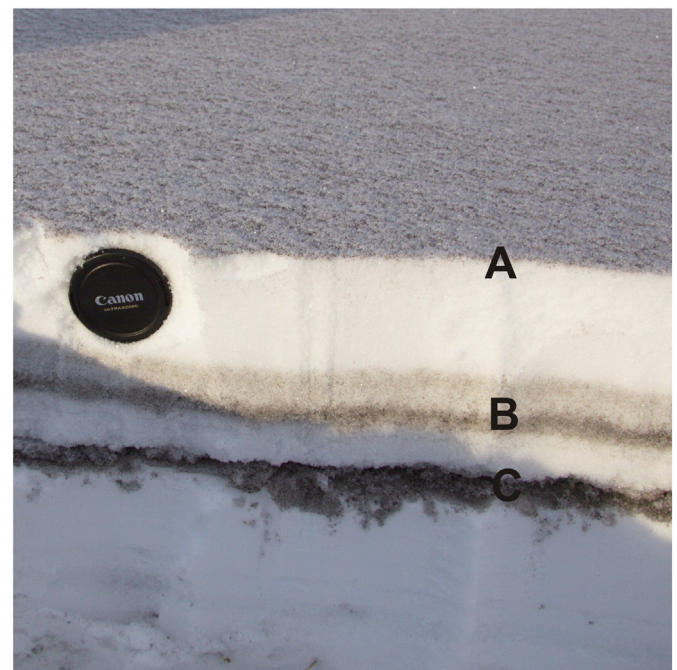


Fig. 4. Cross section through snow showing three ash layers from FTE. Lens cap 77 mm in diameter is used for the scale. Letters A, B and C correspond to the different ash layers, deposited during the initial phase of the eruption. See the text for a detailed description. Photo by S.Ushakov.

Table 1

Major and trace element concentrations in the FTE ash samples compared to the average compositions of the Menyailov and Naboko vent rocks (Volynets et al., 2015), and to the initial stage of the Naboko vent activity (from 2 to 7 December 2012) (results of XRF analyses). Concentrations of major elements are in wt.%, trace elements are in ppm.

	TOLB-A (upper)	TOLB-B (medium)	TOLB-C (lower)	Menyailov vent average	Naboko vent average	Naboko vent, 2-7.12.12	Naboko vent, 15.12.12-1.09.13
SiO ₂	53.62	53.82	53.82	54.71	52.46	52.75	52.46
TiO ₂	1.69	1.80	1.70	1.78	1.96	1.98	1.96
Al ₂ O ₃	16.26	16.66	16.44	16.60	16.33	16.14	16.36
FeO	9.29	9.23	9.20	9.15	10.71	10.58	10.70
MnO	0.16	0.17	0.17	0.17	0.17	0.17	0.17
MgO	3.72	3.31	3.39	3.26	4.14	3.92	4.16
CaO	7.40	7.12	7.21	7.14	7.52	7.66	7.50
Na ₂ O	3.67	3.57	3.80	3.92	3.61	3.68	3.61
K ₂ O	2.37	2.43	2.44	2.55	2.39	2.44	2.38
P ₂ O ₅	0.66	0.45	0.68	0.72	0.70	0.67	0.70
Total	98.85	98.56	98.85	100.00	100.00	100.00	100.00
Mg#	41.64	38.99	39.63	38.85	41.27	39.77	41.40
K ₂ O/MgO	0.55	0.63	0.62	0.67	0.49	0.53	0.49
V	267	228	253	268	290	281	291
Cr	30	13	17	12	34	23	35
Co	30	26	30	25	31	28	31
Ni	25	13	16	12	40	35	40
Zn	115	110	111	119	117	114	117
Rb	63	70	62	72	64	65	64
Sr	323	312	326	335	321	311	322
Y	49	49	50	49	47	45	47
Zr	262	262	259	274	253	247	254
Nb	7	8	7	8	8	9	8
Ba	559	592	558	618	532	539	532
Pb	7	10	9	9	8	8	8
Cu	296	306	294	284	361	370	359

4. Discussion

The first visual observations were made by scientists from the Institute of Volcanology and Seismology FEB RAS after the snowstorm ended, at 19:20 UTC 28 November 2012, from the observation point located about 40 km from FTE vents. An intense glow was visible at night above the Menyailov and Naboko vents (Fig. 7). The Menyailov vent looked more active, with higher explosive activity that emitted hot material to a height of 100–200 m. Later observations were made from

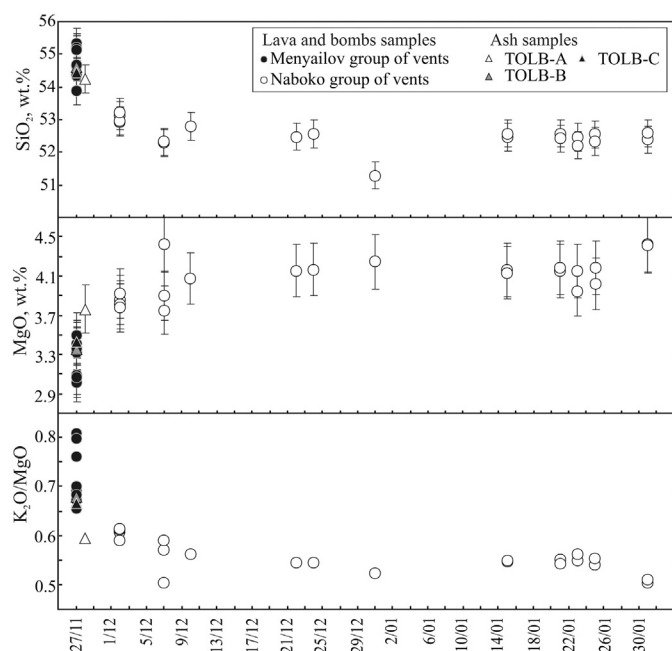


Fig. 6. Temporal variations in lava and ash sample compositions from the beginning of the eruption until the end of January. The horizontal axis represents time. According to Volynets et al. (2015; in this issue), the composition of the Naboko vent lava remained constant and homogeneous from the middle of December until the end of eruption.

00:20 to 01:50 UTC 29 November 2012 during a helicopter overflight (Fig. 8), when, finally, it became possible to survey the eruption site in detail. The Menyailov group of vents continued to have explosive activity via a system of four gushing vents. A large lava flow was produced by this fissure zone; it comprised two streams—the Vodopadny and Leningradsky lava flows (Belousov et al., 2015). At the time of the visual observations, the activity of most of these flows was low; they were slowly advancing only at the frontal parts. Lava flows were about 3–5 m thick at the edges and about 7–12 m thick at the frontal parts. The surface temperature of the peripheral parts of the lava flows was measured during the survey of the peripheral parts of the lava flow on 29 November 2012, by IR pyrometer from the distance of 1–2 m; temperature was 100–200 °C, which was low enough to climb on to the flow to sample the lava. During the helicopter overflight (00:20 to 01:50 UTC 29 November 2012) the Naboko group of vents was located at the southernmost part of the new fissure zone, which intersected Krasny cone. Lava was continuously gushing from the fissure 700 m long; separate explosions also happened at the upper part of the fissure. There were no side levees along the fissure, therefore we assume at the time of observations it had not been active for more than 24 h. This idea is also supported by the fact that the fast moving lava flow produced by this fissure was less than 3 km long at this time. Judging by the VIIRS satellite image it was already 7 km long at 14:49 UTC 29 November 2012.

According to the visual observations, the Menyailov vent activity ceased on 30 November 2012; after that time all activity was concentrated within the Naboko group of vents. The fissure, intersecting Krasny cone, was active by 8 December 2012. Then, the center of activity moved about 800 m to the north, where a new cinder cone was formed. It was active until the end of eruption in September 2013. Detailed evaluation of the eruptive centers and lava flow distributions was done using a satellite image from the Advanced Land Imager (ALI) on the Earth Observing-1 (EO-1) satellite (NASA EO-1 team <http://eo1.gsfc.nasa.gov>) made on 1 December 2012. On that image a thick lava flow is visible (indicated by No. 3 at the image), effusing from the fissure (No. 2) on the slope of Krasny cone (Fig. 9). Also visible is a less intense lava flow (indicated by No. 5) effusing from the eruptive center on the northern side of Krasny cone (No. 4). This center produced several explosive events and lava flows and was active



Fig. 7. Explosive and effusive activity at FTE on 19:20 UTC 28 November 2012. To the left—Menyailov group of vents, to the right—Naboko group of vents. The view is from the north-west from the eruption site, at 40 km distance. Photo by D. Melnikov.

until February 2013; after that, only fumarolic activity was observed there. This cone is located between Krasny and Naboko scoria cones. Naboko cone is not visible as a thermal anomaly in this image, because it had not started to form yet. During the visual observations made on 29 December 2012 we documented only the process of

the beginning of the formation of the scoria cone area, located at the northern edge of Krasny cone (indicated by No. 4 at Fig. 9 and dashed curve at Fig. 8). Thus the Naboko eruptive center comprises a complex morphology made from old (Krasny) and new material (Fig. 10).

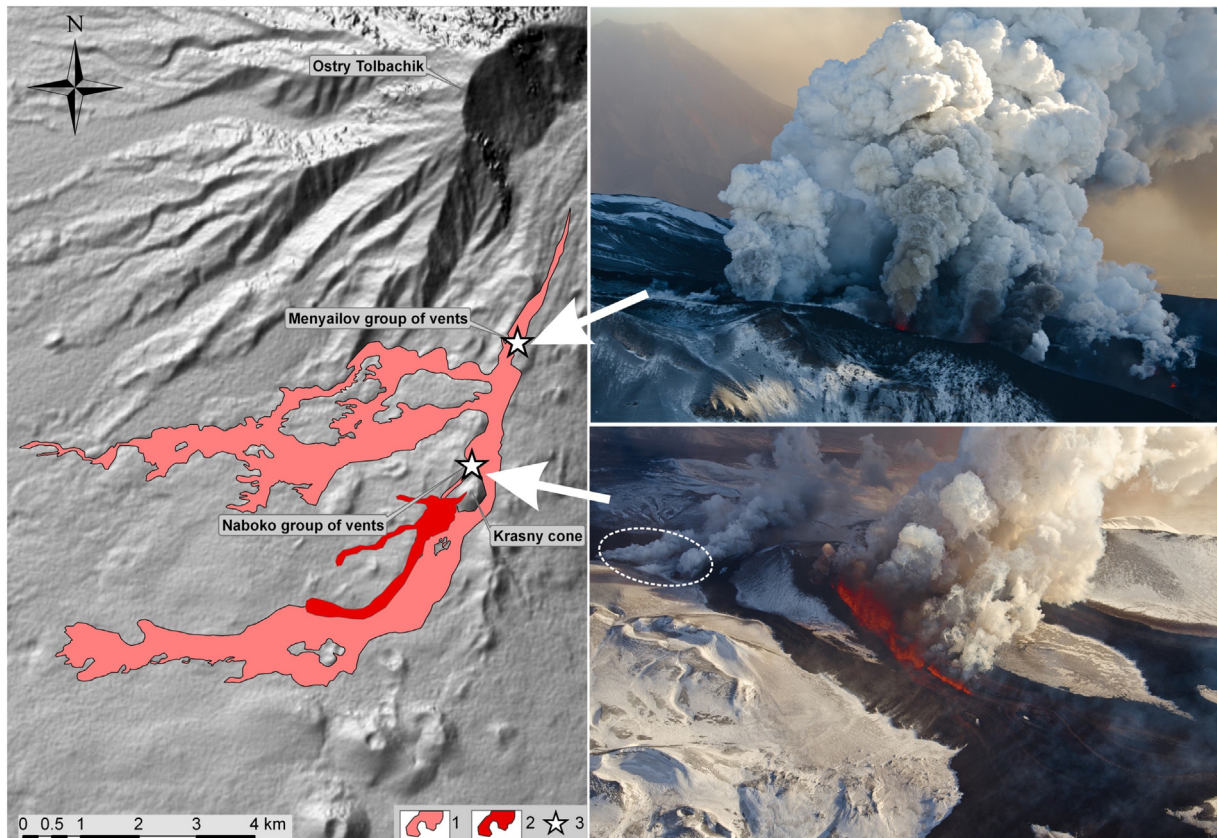


Fig. 8. Map and aerial images of FTE lava flows distribution at 01:00 UTC 29 November 2012. The map is made from visual observations and interpretation of the perspective photographs taken during the helicopter overflight. Legend: 1—lava flows effused from the fissure and from the Menyailov group of vents. The upper stream is named as Vodopadny, the lower—Leningradsky; 2—lava flow started to effuse from the fissure, intersecting Krasny cone; 3—location of the Menyailov group of vents and Naboko group of vents. Arrows point to the photographs of the corresponding group of vents. Dashed contour shows the area where a scoria cone was formed later (shown by the number 4 at Fig. 9). Map and photos by D. Melnikov.

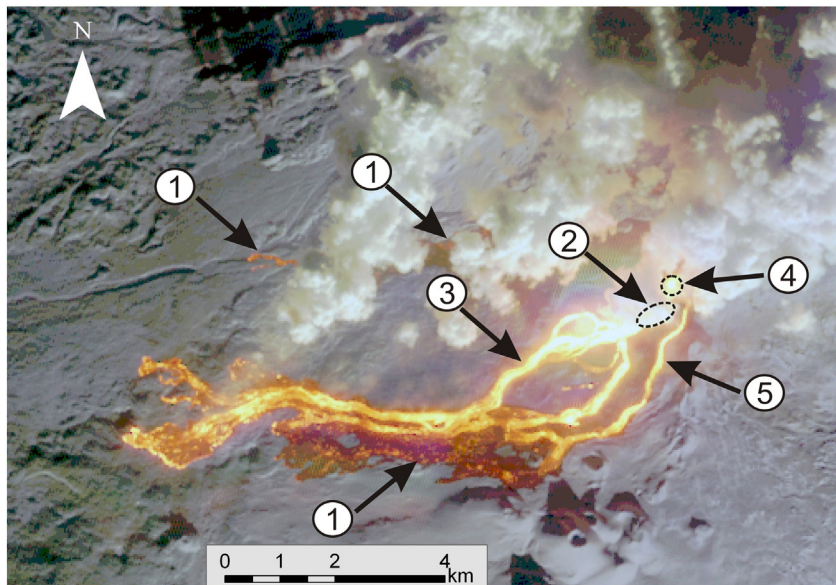


Fig. 9. Satellite image EO-1 ALI (NASA) from 1 December 2012 showing a combination of bands of ALI: Red-10, Green-9, and Blue-8 with wavelength 2.08–2.35 μm , 1.55–1.75 μm , and 1.2–1.3 μm , respectively. Spatial resolution is 30 m. The increase of color intensity towards saturated white corresponds to the higher temperatures. Numbers on the image indicate: 1—lava flows, produced during the period 27–28 November 2012; 2—zone of the fissure that intersected Krasny cone; 3—lava intensively flowing from the fissure, the length of the flow is 10.3 km; 4—eruptive center to the north from Krasny cone; 5—lava flowing from the eruptive center 4, the length of the flow is 5 km.

5. Conclusions

The 2012–2013 Tolbachik eruption occurred in a zone of regional volcanic activity within a composite system of magmatic channels, dykes and storage zones (Fedotov, 1983; Kugaenko et al., 2013; Kugaenko et al., 2015; in this issue; Volynets and Kugaenko, 2015). During the last thousand years at least three other eruptions have taken place exactly within the area of FTE: the 800 year old “New lavas” (Churikova et al., 2015; in this issue), that were produced by eruptive centers on the slope of the Plosky Tolbachik stratovolcano (the outlines of these lava flows are practically identical to the FTE lava flows), Krasny cone in 1740 CE and a cone formed in 1941 CE.



Fig. 10. Photograph of the Naboko eruptive center as viewed from the southwest. Numbers on the image indicate: 1—Krasny cinder cone; 2—fissure that intersected Krasny cone; lava effusions took place here until 8 December 2012; 3—explosive vents, located along the fissure, intersecting Krasny cone; 4—eruptive center, which was active until February 2013; 5—Naboko scoria cone; it was active from December 2012 until September 2013. Dashed lines are used to outline the morphological borders of the structures. Photograph is made by Yu. Demyanchuk on 16 May 2013.

Due to environmental conditions, a complex approach was needed to reconstruct the first 24 h of the eruption. At the beginning of the new eruption, a fissure about 6 km long opened, and the effusion of the lava flow with discharge rate $\sim 440 \text{ m}^3/\text{s}$ accompanied this process. Most likely it happened very fast, during the first 24 h, because 30 h after the onset of the eruption the surface temperature of most parts of the lava flows did not exceed 100–200 $^{\circ}\text{C}$. During this period, the main center from which lava was erupted was the Menyailov vent. The eruption started with effusion of relatively fractionated basaltic trachyandesites. The lower and middle layers of ash (“C” and “B”) are compositionally similar to the Menyailov vent lavas, with SiO_2 53.8–55.4 wt.%, Mg\# 38.15–39.5 and $\text{K}_2\text{O}/\text{MgO}$ ratio 0.61–0.76.

Starting from $\sim 05:00$ to $\sim 09:00$ UTC 28 November 2012 (~ 24 h after the eruption onset) the composition of ash changed to slightly more basic (SiO_2 53.6 wt.%) and Mg-rich (Mg\# 41.6, $\text{K}_2\text{O}/\text{MgO}$ 0.55), similar to the composition of lavas produced by the lower part of the fissure zone at the Naboko vent. Therefore, we propose, that the beginning of the Naboko vent activity is located in the same time interval. Volynets et al. (2015; in this issue) argue that this compositional change can be explained by discharge of a slightly cooler, more fractionated upper part of the magma storage zone before the main storage area began to feed the eruption.

Acknowledgments

Authors are grateful to Tatyana Manevich for providing the ash sample TOLB B for this study. Researches and technical staff of the Institute of Volcanology and Seismology FEB RAS, participated in the field works during the eruption, are thanked for the collaboration and help. Andrey Babansky and Anton Yakushev are thanked for the help in analytical work. We thank Michael Ramsey and the guest editors of the Special issue – Benjamin Edwards, Alexander Belousov and Marina Belousova – for the careful and detailed reviews of the manuscript; their comments and suggestions substantially improved the earlier version of this paper. Work is supported by IVS FEB RAS; RFBR grant 13-05-00760-a; FED RAS grant no. 12-III-A-08-165 (to A.V.).

References

- Belousov, A., Belousova, M., Edwards, B., Volynets, A., Melnikov, D., 2015. Overview of the precursors and dynamics of the 2012–13 basaltic fissure eruption of Tolbachik Volcano, Kamchatka, Russia. *J. Volcanol. Geotherm. Res.* 299, 19–34.
- Brenot, H., Theys, N., Clarisse, L., Van Geffen, J., Van Gent, J., Van Roozendaal, M., Van Der, A.R., Hurtmans, D., Coheur, P.-F., Clerbaux, C., Valks, P., Hedelt, P., Prata, F., Rason, O., Sievers, K., Zehner, C., 2014. Support to Aviation Control Service (SACS): an online service for near-real-time satellite monitoring of volcanic plumes. *Nat. Hazards Earth Syst. Sci.* 14, 1099–1123. <http://dx.doi.org/10.5194/nhess-14-1099-2014>.
- Churikova, T.G., Gordeychik, B.N., Edwards, B.R., Ponomareva, V.V., Zelenin, E., 2015. The Tolbachik volcanic complex: a review of the petrology, volcanology and eruption history prior to the 2012–2013 eruption. *J. Volcanol. Geotherm. Res.* (in this issue).
- Dvigalo, V.N., Svirid, I.Yu., Shevchenko, A.V., 2014. The first quantitative estimates of parameters for the Tolbachik Fissure Eruption of 2012–2013 from aerophotogrammetric observations. *J. Volcanol. Seismol.* 8 (5), 261–268.
- Fedotov, S.A. (Ed.), 1983. *The Great Tolbachik Fissure Eruption; Geological and Geophysical Data 1975–1976*. Cambridge Univ. Press, Cambridge, United Kingdom (353 p).
- Fedotov, S.A., Flerov, G.B., Chirkov, A.M. (Eds.), 1984. *The 1975–1976 Large Tolbachik Fissure Eruption in Kamchatka*. Nauka, Moscow (in Russian with English abstract).
- Gordeev, E.I., Muravev, Ya.D., Samoilenko, S.B., Volynets, A.O., Melnikov, D.V., Dvigalo, V.N., 2013. The Tolbachik Fissure Eruption of 2012–2013: preliminary results. *Dokl. Earth Sci.* 452 (part 2), 1046–1050. <http://dx.doi.org/10.1134/S1028334X13100103>.
- Harris, A., 2013. *Thermal Remote Sensing of Active Volcanoes: A User's Manual*. Cambridge University Press.
- Harris, A.J., Flynn, L.P., Keszthelyi, L., Mougini-Mark, P.J., Rowland, S.K., Resing, J.A., 1998. Calculation of lava effusion rates from Landsat TM data. *Bull. Volcanol.* 60 (1), 52–71.
- Inbar, M., Gilichinsky, M., Melekestsev, I., Melnikov, D., Zaretskaya, N., 2011. Morphometric and morphological development of Holocene cinder cones: a field and remote sensing study in the Tolbachik volcanic field, Kamchatka. *J. Volcanol. Geotherm. Res.* 201 (1), 301–311. <http://dx.doi.org/10.1016/j.jvolgeores.2010.07.013>.
- Kugaenko, Y.A., Saltykov, V.A., Gorbatiykov, A.V., Stepanova, M.Y., 2013. Deep structure of the North Vent Area, Great Tolbachik Fissure Eruption of 1975–1976, Kamchatka: evidence from low-frequency microseismic sounding. *J. Volcanol. Seismol.* 7 (5), 313–327.
- Kugaenko, Yu.A., Titkov, N.V., Saltykov, V.A., 2014. Crustal deformation and seismic activation preceding the 2012–13 fissure eruption at Tolbachik Volcanic Zone, Kamchatka. *Proceedings of the 8th Biennial Workshop on Japan–Kamchatka–Alaska Subduction Processes: Finding Clues for Science and Disaster Mitigation from International collaboration (JKASP-2014)*. Hokkaido University, Sapporo, Japan.
- Kugaenko, Yu., Titkov, N., Saltykov, V., 2015. Constraints on unrest in the Tolbachik volcanic zone in Kamchatka prior the 2012–13 flank fissure eruption of Plosky Tolbachik volcano from local seismicity and GPS data. *J. Volcanol. Geotherm. Res.* <http://dx.doi.org/10.1016/j.jvolgeores.2015.05.020> (in this issue).
- Parker, M.J., Weber, A.H., Buckley, R.L., 2004. *Short Term Climatological Wind Data as a Tool for Wind Forecasting*. Weather and Forecasting, AMS, Boston, MA.
- Pieri, D., Abrams, M., 2004. ASTER watches the world's volcanoes: a new paradigm for volcanological observations from orbit. *J. Volcanol. Geotherm. Res.* 135 (1), 13–28.
- Schroeder, W., Oliva, P., Giglio, L., Csiszar, I.A., 2014. The New VIIRS 375 m active fire detection data product: algorithm description and initial assessment. *Remote Sens. Environ.* 143, 85–96.
- Senyukov, S.L., Nuzhdina, I.N., Droznina, S.Ya., Garbuzova, V.T., Kozhevnikova, T.Yu., Sobolevskaia, O.V., Nazarova, Z.A., Bliznetsov, V.E., 2015. Seismic monitoring of the Plosky Tolbachik eruption in 2012–13 (Kamchatka peninsula, Russia). *J. Volcanol. Geotherm. Res.* <http://dx.doi.org/10.1016/j.jvolgeores.2015.07.026> (in this issue).
- Volynets, A., Kugaenko, Y., 2015. Integration of geochemical, petrological and seismic data for the study of volcanic plumbing system of the 1975–76 Tolbachik fissure eruption. 26th IUGG 2015 General Assembly, Prague, Czech Republic, 22 June – 2 July 2015.
- Volynets, A., Melnikov, D., Yakushev, A., 2013. First data on composition of the volcanic rocks of the IVS 50th anniversary Fissure Tolbachik Eruption. *Dokl. Earth Sci.* 452, 953–957. <http://dx.doi.org/10.1134/S1028334X13090201>.
- Volynets, A., Edwards, B., Melnikov, D., Yakushev, A., Griboedova, I., 2015. Monitoring of the volcanic rock compositions during the 2012–2013 fissure eruption at Tolbachik volcano, Kamchatka. *J. Volcanol. Geotherm. Res.* <http://dx.doi.org/10.1016/j.jvolgeores.2015.07.014> (in this issue).
- Wright, R., Blackett, M., Hill-Butler, C., 2015. Some observations regarding the thermal flux from Earth's erupting volcanoes for the period of 2000 to 2014. *Geophys. Res. Lett.* 42. <http://dx.doi.org/10.1002/2014GL061997>.